

## Comparing Different Approaches To Intergranular Stress Modeling

**T. Mede, S. El Shawish**

Jožef Stefan Institute

Jamova cesta 39

SI-1000, Ljubljana, Slovenia

timon.mede@ijs.si, samir.elshawish@ijs.si

### ABSTRACT

Predicting how cracks get formed within a polycrystalline material under mechanical load requires the knowledge of intergranular normal stresses in it. Two analytical models for estimating them are presented and their results compared, to better understand the significance of the approximations, upon which each of the models is based.

### 1 INTRODUCTION

Polycrystalline materials, such as metals, alloys and various ceramics, are composed of grains, which are tiny crystals of different shapes and sizes, each with randomly oriented crystal structure. When external mechanical load is applied to such aggregate, cracks might develop along the grain boundaries (GBs) that separate different grains. These cracks can compromise the object's structural integrity and shorten its service time, but whether or not they form, depends on the amplitude of stresses induced between different grains and their exact microstructure. The basic mechanism is that when intergranular normal stress (INS) exceeds the local GB strength, a microcrack appears at its position, and when those become dense enough, they can merge into observable, macroscopic cracks. Both the INS and GB strength are local quantities in a sense that they depend on the exact location of the GB within the aggregate and/or environmental conditions, such as its corrosiveness or radiation exposure.

Hence, the knowledge of local GB stresses is essential for predicting the initiation of microcracks. For a particular aggregate and loading, these stresses can be accurately estimated by numerical simulations [relying, for instance, on the finite-element (FE) method], but those are computationally demanding and time-consuming due to a large number of grains in a macroscopic object (for which the constitutive equations need to be solved), as well as impractical since they require the knowledge of the exact microstructure of the aggregate. This information is redundant if the goal is to estimate the probability that a crack will develop in a certain industrial component under a specific loading, because the configuration of all the grains in each individual piece [including the grain shapes, their crystallographic orientations and presence of possible defects, such as voids, inclusions, ...] is stochastic.

Alternatively, the (average) neighborhood of the GB can be modeled, which allows us to derive an (approximate) analytic expression for the induced stress on it. Since the amount of stress a GB can withstand before it cracks should not depend on its orientation, GBs can be classified into different GB types. All GBs of the same type should have the same GB strength,

while their GB stresses can differ, producing a unique INS distribution for each type. In principle, GB strength and the corresponding GB type depend on the complete neighbourhood of the GB. But since the effect of surrounding grains gradually diminishes with their distance from the GB, the two adjacent grains are considered the most relevant, and in first approximation we can neglect all others. Each GB type in a chosen material can thus be specified by just 5 parameters (e.g., the GB-normal vector expressed in crystallographic systems of both adjacent grains  $[(a, b, c)$  and  $(d, e, f)]$ , and the twist angle  $\Delta\omega$  between their crystal lattices about the GB normal), while additional 2 degrees of freedom (orientation of the GB plane with respect to external stress) are needed to define a specific GB within that type.

## 2 THE MODELS

To obtain GB-normal<sup>1</sup> stress  $\sigma_{zz}$ , constitutive equations of the *generalized Hooke's law*

$$\epsilon_{ij}^{(n)} = \sum_{k,l \in \{x,y,z\}} \tilde{s}_{ijkl}^{(n)} \sigma_{kl}^{(n)}, \quad i, j = x, y, z \quad (1)$$

need to be solved for the two grains enclosing the GB. The 12 coupled equations relate the components of symmetric strain ( $\epsilon_{ij}^{(n)}$ ) and stress ( $\sigma_{kl}^{(n)}$ ) tensors in each grain ( $n = 1, 2$ ) through the local, rank 4 compliance tensor ( $\tilde{s}_{ijkl}$ ). They are accompanied by 6 “*inner*” *boundary conditions* at the GB:

*stress continuity across the GB*

$$\sigma_{xz}^{(1)} = \sigma_{xz}^{(2)}, \quad \sigma_{yz}^{(1)} = \sigma_{yz}^{(2)}, \quad \sigma_{zz}^{(1)} = \sigma_{zz}^{(2)}, \quad (2)$$

*strain compatibility across the GB*

$$\epsilon_{xx}^{(1)} = \epsilon_{xx}^{(2)}, \quad \epsilon_{xy}^{(1)} = \epsilon_{xy}^{(2)}, \quad \epsilon_{yy}^{(1)} = \epsilon_{yy}^{(2)}. \quad (3)$$

Another 6 relations are thus needed to be able to solve the system of equations for all the variables. These “*outer*” *boundary conditions* should specify, how investigated pair of grains is deformed as a whole, when the aggregate is put under a specific external loading  $\Sigma$ :

$$\begin{aligned} V_1 \epsilon_{xx}^{(1)} + V_2 \epsilon_{xx}^{(2)} &= (V_1 + V_2) \bar{\epsilon}_{xx}^b, & V_1 \epsilon_{yz}^{(1)} + V_2 \epsilon_{yz}^{(2)} &= (V_1 + V_2) \bar{\epsilon}_{yz}^b, \\ V_1 \epsilon_{yy}^{(1)} + V_2 \epsilon_{yy}^{(2)} &= (V_1 + V_2) \bar{\epsilon}_{yy}^b, & V_1 \epsilon_{xz}^{(1)} + V_2 \epsilon_{xz}^{(2)} &= (V_1 + V_2) \bar{\epsilon}_{xz}^b, \\ V_1 \epsilon_{zz}^{(1)} + V_2 \epsilon_{zz}^{(2)} &= (V_1 + V_2) \bar{\epsilon}_{zz}^b, & V_1 \epsilon_{xy}^{(1)} + V_2 \epsilon_{xy}^{(2)} &= (V_1 + V_2) \bar{\epsilon}_{xy}^b, \end{aligned} \quad (4)$$

where  $\bar{\epsilon}_{ij}^b$  is the *average strain of a specific bicrystal pair* and  $V_1$  and  $V_2$  are the volumes of the corresponding grains. If  $\bar{\epsilon}_{ij}^b$  were known, Eqs. (1)–(4) would provide an exact solution for the induced stress  $\sigma_{zz}$  at the chosen GB.<sup>2</sup> Unfortunately it is impossible to determine, how the macroscopic stress  $\Sigma$  is transferred to a certain pair of grains without solving the equations for all the grains in the aggregate. Finite element numerical simulations do exactly that and produce accurate results, but since they require as an input the information about the exact configuration of all the grains in the aggregate, any general conclusions are difficult to make.

<sup>1</sup>Local (GB) coordinate system with  $z$ -axis directed along the GB normal is chosen.

<sup>2</sup>Neglecting the fact, that in realistic case neither the grains are perfectly homogeneous (due to the presence of defects) nor are the corresponding strain and stress tensor constant within each grain.

Alternative approach is to make instead some reasonable assumptions about the deformation ( $\bar{\epsilon}_{ij}^b$ ) of a selected grain pair. Essentially, this can be seen as the modeling of “outer” boundary conditions. Strictly speaking, the deformation of each grain depends on its precise location within the polycrystalline aggregate, but the combined effect of all the surrounding grains can be successfully decomposed into various contributions according to their relevance (from more to less important: GB orientation with respect to external loading, GB type and GB neighborhood). Perturbative treatment allows us to gradually increase the complexity of the model, neglecting the specifics of more distant grains (i.e., modeling their effect in less detail by using only macroscopic material properties) and focusing primarily on the structure of grains closest to the investigated GB (Saint Venant’s principle). This represents a compromise between the model’s simplicity and its accuracy. In the simplest approximation, the (inhomogeneity of the) neighborhood of a chosen GB can be neglected entirely, in which case the only relevant degree of freedom is the orientation of the GB plane and the induced stress on it is equal to external stress ( $\sigma_{ij} = \Sigma_{ij}$ ). This corresponds to isotropic case. In the next-order iteration, the procedure allows us to reduce the problem to a pair of grains embedded in a homogeneous and isotropic elastic medium with average bulk properties. This is the subject of the present study.

## 2.1 Bicrystal model

Simplest such case is the *bicrystal model*, based on the postulate, that each pair of grains deforms the same as bulk material of equal dimensions would if subjected to the same external loading, i.e., matching  $\bar{\epsilon}_{ij}^b$  to the macroscopic strain  $\bar{\epsilon}_{ij}$  of the polycrystalline aggregate. This allows us to express the strain of a bicrystal pair in terms of the average Young’s modulus  $\bar{E}$  and Poisson’s ratio  $\bar{\nu}$  of the material

$$\bar{\epsilon}_{ij}^b = \bar{\epsilon}_{ij} = \frac{1 + \bar{\nu}}{\bar{E}} \Sigma_{ij} - \frac{\bar{\nu}}{\bar{E}} (\text{Tr } \Sigma) \delta_{ij} . \quad (5)$$

For average grains this assumption works well, but the stiffer or softer the grains in the pair are, the worse the results get. For a very stiff GB the amplitude of induced stress is smaller than model prediction (for both tensile and compressive loadings), since the true grains should deform less than the bulk, while for a very soft GB the effect is the opposite. Consequently, the estimated standard-deviation curve as a function of GB stiffness is unrealistically steep [1].

For demonstration purposes cubic lattice symmetry is assumed throughout this paper. In that case, the compliance tensor components in each grain depend on just 3 parameters ( $S_{11}$ ,  $S_{12}$  and  $S_{44}$ )

$$s_{mmmm} := S_{11} , \quad m = 1, 2, 3 , \quad (6)$$

$$s_{mnmn} = s_{mnnm} := \frac{S_{44}}{4} , \quad m, n \neq m = 1, 2, 3 , \quad (7)$$

$$s_{mmnn} := S_{12} , \quad m, n \neq m = 1, 2, 3 , \quad (8)$$

$$s_{mnop} := 0 , \quad \text{otherwise} , \quad (9)$$

for the (local) directions 1, 2, 3 aligned with crystallographic axes of the grain.<sup>3</sup> Similarly, also

<sup>3</sup>To relate  $s_{mnop}$  to  $\tilde{s}_{ijkl}$ , transformation to GB system must be performed (introducing 3 Euler angles, or equivalently, GB-normal direction  $(h, k, l)$ , and a twist angle  $\omega$  about it).

$\bar{E}$  and  $\bar{\nu}$  are then only functions of  $S_{11}$ ,  $S_{12}$  and  $S_{44}$

$$\bar{E} = \frac{9KG}{3K + G}, \quad (10)$$

$$\bar{\nu} = \frac{3K - 2G}{2(3K + G)} = \frac{1 - (S_{11} + 2S_{12})\bar{E}}{2}, \quad (11)$$

through their dependence on the corresponding compression and shear elastic moduli

$$K = \frac{1}{3(S_{11} + 2S_{12})}, \quad (12)$$

$$G = \begin{cases} 8(S_{11} + 2S_{12})(S_{11} - S_{12})S_{44}G^3 + (5S_{11} + S_{12})S_{44}G^2 - (7S_{11} + 11S_{12})G = 1 \\ G > 0 \end{cases}. \quad (13)$$

However, the system of coupled linear equations in Eq. (1) with boundary conditions (2)–(5) and grains of equal size ( $V_1 = V_2$ ) is even for cubic lattice symmetry too complicated to be solved analytically and its solution presented in a closed form for a general case. Hence, we need to deal with it numerically for a chosen material ( $S_{11}$ ,  $S_{12}$ ,  $S_{44}$ ), GB type ( $a$ ,  $b$ ,  $c$ ,  $d$ ,  $e$ ,  $f$  and  $\Delta\omega$ ), GB orientation, and loading ( $\Sigma$ ). To obtain an analytic expression for  $\sigma_{zz}$  on a particular GB, which would allow us to quickly estimate the INS distributions without having to rely on numerical computations, thus requires some further approximations.

## 2.2 Buffer-grain model

The main problem of bicrystal model lies with the assumption, that bicrystal pair deforms as bulk material. This is manifestly not true when grains in the pair are either very stiff or very soft. To relax that constraint and temper the GB's response, “*buffer*” grains (with bulk properties  $\bar{E}$  and  $\bar{\nu}$ ) are introduced. Together with GB grains they form a set of mutually orthogonal linear (1D) chains along the GB normal and perpendicular to it. Entire chains (not solely the bicrystal pair) are then supposed to deform as if they were made from bulk material. Schematic depiction of the model [2] is presented in Fig. 1.

Additional trouble with bicrystal model is that analytical expression for  $\sigma_{zz}$  is not available. The main obstacle is the mixed nature of boundary conditions — some apply to strains while others to stresses, where both sets of variables are related through the Hooke's law. Because the proportionality factor [compliance-tensor components] can be quite complicated, the resulting expressions for the GB stresses are extremely tedious. To avoid that, we do not invoke the complete set of (inner) boundary conditions. In particular, we shall henceforth neglect the strain compatibility across the GB [cf. Eq. (3)], and assume instead that shear stresses in both grains are equal to the respective components of external stress tensor,

$$\sigma_{ij}^{(1)} = \sigma_{ij}^{(2)} := \Sigma_{ij}, \quad i \neq j. \quad (14)$$

The number of unknowns is thus reduced to five ( $\sigma_{xx}^{(1)}$ ,  $\sigma_{yy}^{(1)}$ ,  $\sigma_{xx}^{(2)}$ ,  $\sigma_{yy}^{(2)}$ ,  $\sigma_{zz} := \sigma_{zz}^{(1)} = \sigma_{zz}^{(2)}$ ). It is matched by the equal number of boundary conditions constraining the lengths of the main (axial) chain with  $L+2$  grains, and four transverse (side) chains with  $L_t+1$  grains. For simplicity, all grains are also assumed to be of the same size.

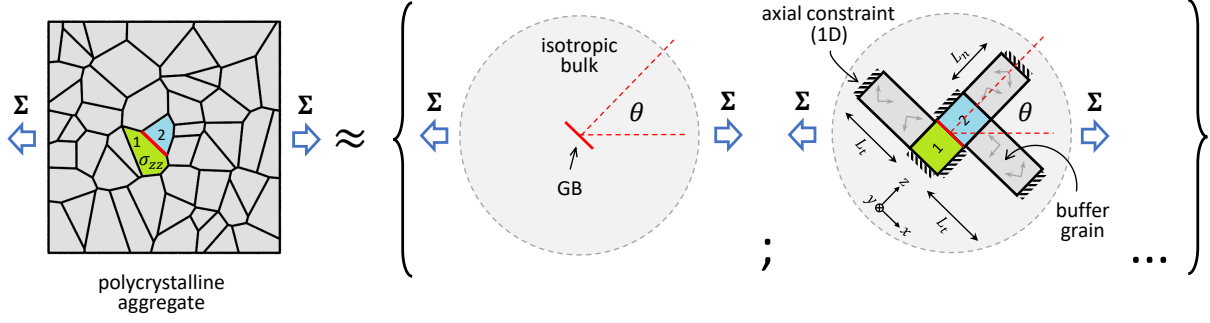


Figure 1: Perturbative approach for estimating GB-normal stresses  $\sigma_{zz}$  in a polycrystalline aggregate under uniform loading  $\Sigma$ . At each order of perturbation, GB neighborhood is considered in more details. First two orders are shown, i.e., isotropic case, which does not distinguish between different GB types, and bicrystal model (whose response is moderated by buffer grains). The grains in different chains deform independently of each other (violating strain compatibility across the GB). For simplicity, the two side chains in  $y$ -direction are not shown. Second order approximation [2] reduces to isotropic model for infinitely long chains (in  $L_n, L_t \rightarrow \infty$  limit).

With this ansatz a simple analytical solution for local GB stress  $\sigma_{zz}$  on any GB of any GB type can be obtained for arbitrary uniform external loading and/or polycrystalline material<sup>4</sup>

$$\sigma_{zz} = C_n \Sigma_{zz} + C_t (\Sigma_{xx} + \Sigma_{yy}) , \quad (15)$$

where all the dependence on GB orientation (angles  $\theta$  and  $\psi$ ) is contained in components of external stress tensor expressed in a (local) GB coordinate system ( $\Sigma_{ij}$ ), while any reference to material properties ( $S_{ij}$ ) and GB type ( $a, b, c, d, e, f$ ), except the twist angle  $\Delta\omega = \omega_2 - \omega_1$ , which has been averaged over and thus integrated out, is stored in coefficients

$$C_n = \frac{(1 + (2L_t + s')E_{12})(L_n + 2s' + 4(L_t + s')E_{12}) + (2L_n L_t + L_n s' - 2s'^2)E_{12} + (L_n + 2s')\Delta_{12}}{(1 + (2L_t + s')E_{12})(L_n + 2s' + 4(L_t + s') + (2L_n L_t + L_n s' - 2s'^2)E_{12}) + (L_n + 2s' + 4(L_t + s'))\Delta_{12}} , \quad (16)$$

$$C_t = \frac{(1 + (2L_t + s')E_{12})(2(L_t + s') - 2(L_t + s')E_{12}) + 2(L_t + s')\Delta_{12}}{(1 + (2L_t + s')E_{12})(L_n + 2s' + 4(L_t + s') + (2L_n L_t + L_n s' - 2s'^2)E_{12}) + (L_n + 2s' + 4(L_t + s'))\Delta_{12}} \\ = \frac{1}{2}(1 - C_n) . \quad (17)$$

All the quantities appearing in  $C_n$  and  $C_t$  are dimensionless, with  $s'$  denoting

$$s' := \bar{E}(S_{11} + 2S_{12}) = 1 - 2\bar{\nu} , \quad (18)$$

and  $E_{12}$  the effective GB stiffness, while  $\Delta_{12}$  is some new quantity measuring the deviation from a single-grain scenario [the  $(abc)$ - $(abc)$  GB type], for which  $\Delta_{12}$  exactly vanishes,

$$E_{12} := \frac{2\bar{E}^{-1}}{E_{abc}^{-1} + E_{def}^{-1}} , \quad (19)$$

$$\Delta_{12} := \frac{4 E_{abc}^{-1} E_{def}^{-1}}{(E_{abc}^{-1} + E_{def}^{-1})^2} - 1 = (E_{12} \bar{E})^2 E_{abc}^{-1} E_{def}^{-1} - 1 . \quad (20)$$

Both are functions of inverse Young's moduli  $E_{abc}^{-1}$  and  $E_{def}^{-1}$  along the GB-normal direction in either grain,

$$E_{hkl}^{-1} := \tilde{s}^{(hkl)} = S_{11} - 2S_0 \frac{(hk)^2 + (hl)^2 + (kl)^2}{(h^2 + k^2 + l^2)^2} , \quad (21)$$

<sup>4</sup>In fact, this can be done not only for cubic grains but even for the most general (triclinic) lattice symmetry [2].

where  $S_0 := S_{11} - S_{12} - \frac{S_{44}}{2} = \frac{S_{44}}{2}(A - 1)$  is proportional to anisotropy of the material expressed by its Zener index  $A$  (with  $A = 1$  referring to the isotropic case).

The first two statistical moments (i.e., the mean value and standard deviation) of the corresponding INS distribution can also be easily derived

$$\langle \sigma_{zz} \rangle := \frac{1}{4\pi} \int_0^{2\pi} \int_0^\pi \sigma_{zz} \sin \theta \, d\theta \, d\psi = \frac{\text{Tr}(\Sigma)}{3}, \quad (22)$$

$$\begin{aligned} s(\sigma_{zz}) &:= \sqrt{\langle (\sigma_{zz} - \langle \sigma_{zz} \rangle)^2 \rangle} = \sqrt{\frac{1}{4\pi} \int_0^{2\pi} \int_0^\pi (\sigma_{zz} - \langle \sigma_{zz} \rangle)^2 \sin \theta \, d\theta \, d\psi} = \frac{2\Sigma_{mis}}{3\sqrt{5}} \times |C_n - C_t| \\ &= \frac{2\Sigma_{mis}}{3\sqrt{5}} \times \\ &\times \left| \frac{(1 + (2L_t + s')E_{12})(L_n - 2L_t + 6(L_t + s')E_{12} + (2L_n L_t + L_n s' - 2s'^2)E_{12}) + (L_n - 2L_t)\Delta_{12}}{(1 + (2L_t + s')E_{12})(L_n + 2s' + 4(L_t + s') + (2L_n L_t + L_n s' - 2s'^2)E_{12}) + (L_n + 2s' + 4(L_t + s'))\Delta_{12}} \right|. \end{aligned} \quad (23)$$

The important thing to note is that they both scale with rotation-invariant functions of external-stress components,

$$\text{Tr} \Sigma := \Sigma_{xx} + \Sigma_{yy} + \Sigma_{zz}, \quad (24)$$

and von Mises external stress

$$\Sigma_{mis} := \sqrt{\Sigma_{xx}^2 + \Sigma_{yy}^2 + \Sigma_{zz}^2 - (\Sigma_{xx}\Sigma_{yy} + \Sigma_{xx}\Sigma_{zz} + \Sigma_{yy}\Sigma_{zz}) + 3(\Sigma_{xy}^2 + \Sigma_{xz}^2 + \Sigma_{yz}^2)}, \quad (25)$$

respectively, which both retain the same form in all coordinate systems. The prefactor in front of  $|C_n - C_t|$  in Eq. (23) is precisely the standard deviation  $s(\sigma_{zz})$  for the isotropic case.

### 3 THE RESULTS

In this section we compare the predictions of both models, to investigate how applying different assumptions (boundary conditions, use of buffer grains, ...) affects their results. In particular, we study the first two statistical moments of INS distributions, the relevance of effective GB-stiffness parameter  $E_{12}$  (and  $\Delta_{12}$ ), and the dependence on the twist angle  $\Delta\omega$ , for various GB types.

Both models not only predict the correct mean value  $\langle \sigma_{zz} \rangle = \text{Tr} \Sigma / 3$  for normal-stress distributions of different GB types, but they also prove the significance of effective GB-stiffness parameter [defined in Eq. (19)], revealing a very strong correlation between  $E_{12}$  and the width of associated INS distribution  $s(\sigma_{zz})$ , see Fig. 2. All results are displayed for  $\gamma$ -Fe and Li grains (see Table 1) under *uniaxial* tensile loading.<sup>5</sup> Using a more general uniform loading would result only in numerically different normalization factors for the first two statistical moments; cf. Eqs. (24)–(25).

Table 1: Material properties of two selected polycrystallines with cubic lattice symmetry: their elastic compliance constants  $S_{ij}$  (in Voigt notation) and the corresponding Zener elastic anisotropy indices  $A = 2(S_{11} - S_{12})/S_{44}$  are listed.

Material	$S_{11}$ [GPa <sup>-1</sup> ]	$S_{12}$ [GPa <sup>-1</sup> ]	$S_{44}$ [GPa <sup>-1</sup> ]	$A$
$\gamma$ -Fe	$9.94 \times 10^{-3}$	$-3.85 \times 10^{-3}$	$8.20 \times 10^{-3}$	3.37
Li	0.333	-0.153	0.114	8.52

<sup>5</sup>In this specific case the components of external stress in a local GB system ( $\Sigma_{ij}$ ) become functions of 2 spherical angles: inclination  $\theta$  and twist rotation  $\phi$ . For multiaxial loadings an additional angle  $\psi$  becomes relevant.

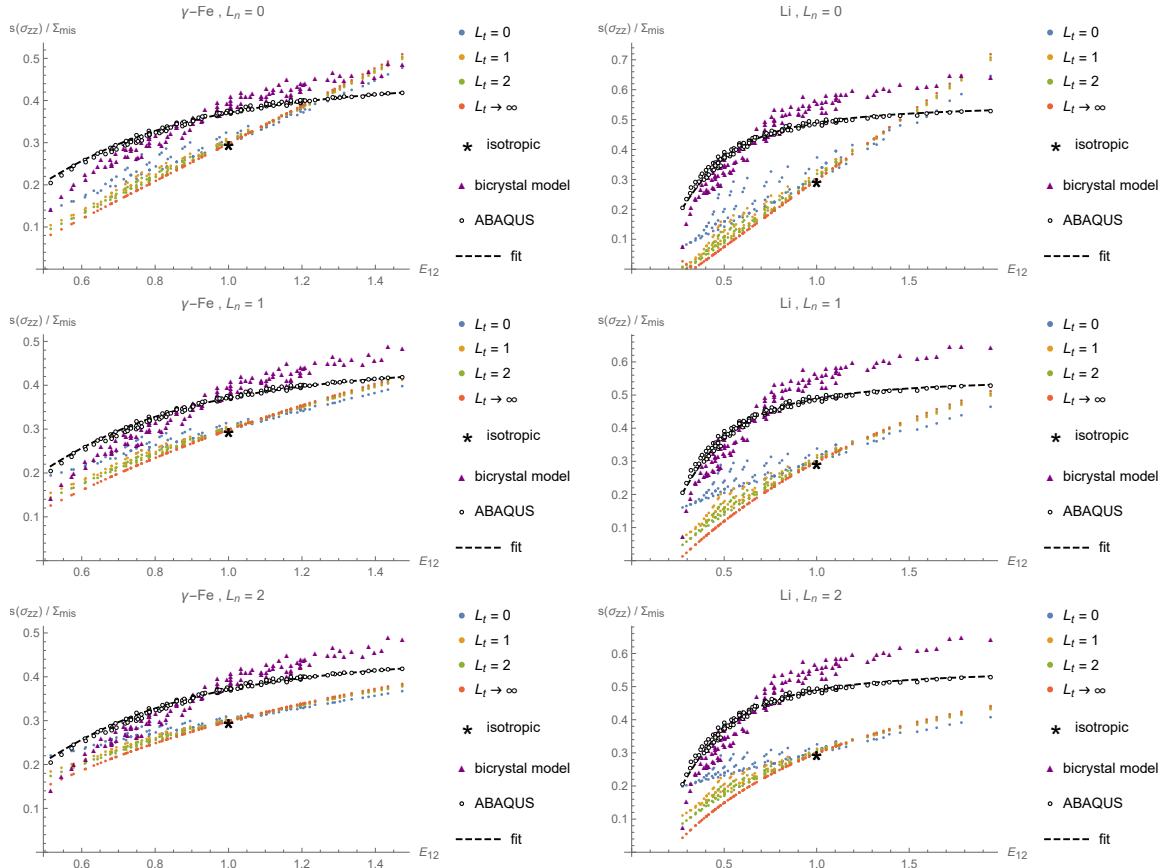


Figure 2: Standard deviation of  $\sigma_{zz}$  distribution for two selected cubic materials, various choices of chain lengths  $L_n$  and  $L_t$ , and different GB types (each corresponding to a distinct value of  $E_{12}$ ); cf. Eq. (23).  $L_n, L_t \rightarrow \infty$  limit corresponds to the isotropic case and reduces to a single point (denoted by  $\star$ ). For comparison, the results of bicrystal model and FE simulations with ABAQUS code are added. Both are obtained for unspecified (random) twist angle to facilitate a comparison with buffer-grain model, which is averaged over  $\Delta\omega$ . Black dashed line represents a numerical fit of FE results [1], that neglects any possible effect of  $\Delta_{12}$ .

The relevance of  $E_{12}$  parameter (as a good quantity) for specifying the  $\sigma_{zz}$  fluctuations in materials with cubic symmetry has been identified already with numerical (FE) simulations [1]. However, since in that analysis also some GB types have been considered which share a common  $E_{12}$  value,<sup>6</sup> it was clearly visible that  $s(\sigma_{zz})$  is not an infinitely sharp function of  $E_{12}$ . The reason for that was not understood at the time — the possible explanations ranged from insufficient numerical accuracy [too small aggregate and thus poor statistics] to failure of proposed model description.

Comparison with analytical models in Fig. 2 shows that produced trends are similarly monotonic [although with different slopes], while the new parameter  $\Delta_{12}$  [see Eq. (23)] can (at least qualitatively) explain the spread of  $s(\sigma_{zz})$ , i.e., the deviation from predicted monotonically increasing curve. Note that in bicrystal model the spread of  $s(\sigma_{zz})$  values at the same  $E_{12}$  is much larger than for ABAQUS results, while in buffer-grain model the effect decreases with the growing  $L_t$  and for long enough side chains resembles the situation in realistic case, see Fig. 2. This gives us hope that the parameter  $\Delta_{12}$  can be used even for quantitative predictions.

The results in Fig. 2 also demonstrate that the agreement is best for  $L_n = 2$  and  $L_t \neq 0$ , since the standard deviation predicted by our analytical model should only increase in realistic case, i.e., once the fluctuations of GB neighborhood are properly taken into account. Hence, the model prediction should be everywhere below the ABAQUS curve.

Integrating out the twist-angle degrees of freedom makes the expressions in Eqs. (15)–(17) and (23) only an approximate<sup>7</sup> (but significantly more condensed) solution of the model, which is such that it still preserves the correct mean value  $\langle \sigma_{zz} \rangle$  [cf. Eq. (22)]. To illustrate the effect of the twist angle, we present  $s(\sigma_{zz})$  as a function of  $\Delta\omega$  for six selected GB types. Three of them correspond to the same  $E_{12}$  value, while other three are independent of the twist angle. The results in Fig. 3 refer to the bicrystal model, but also in buffer-grain model the functional dependence is similar.

## 4 CONCLUSIONS

Two simplified models for estimating intergranular normal stresses and their distributions on various grain-boundary types in polycrystalline materials under uniform external loading are presented. Comparison between them shows the effect of “inner” and “outer” boundary conditions for strains on the (width of) INS distributions. Both models exhibit similar dependence on the twist angle and prove the relevance of the GB-stiffness parameter. These results justify the approach taken in Ref. [2] for deriving an approximate analytical model of GB-normal stresses.

For above results to be directly useful in the probabilistic modeling of grain-boundary-damage initiation (e.g., for intergranular stress-corrosion cracking, intergranular fatigue cracking or grain-boundary sliding in various structural materials), they would have to agree with a more realistic situation, that properly takes into account the effect of more distant grains, e.g., with the outcome of numerical, finite element simulations, in which the exact configuration of the entire aggregate is considered. The influence of surrounding grains can be successfully emulated by performing a convolution of modeled INS distribution with Gaussian fluctuations; cf. [2].

<sup>6</sup>Specifically, that happened when the chosen GB type was such that for at least one of the grains the GB normal was along the (101), (112) or (314) directions, preselected from the stereographic triangle.

<sup>7</sup>With the exception of (100)-(100), (111)-(111) and (100)-(111) GBs, for which the true  $\sigma_{zz}$  is independent of  $\Delta\omega$ , and thus the integration over the twist angle is irrelevant. In these cases the solution produced by Eqs. (15)–(17) is exact.



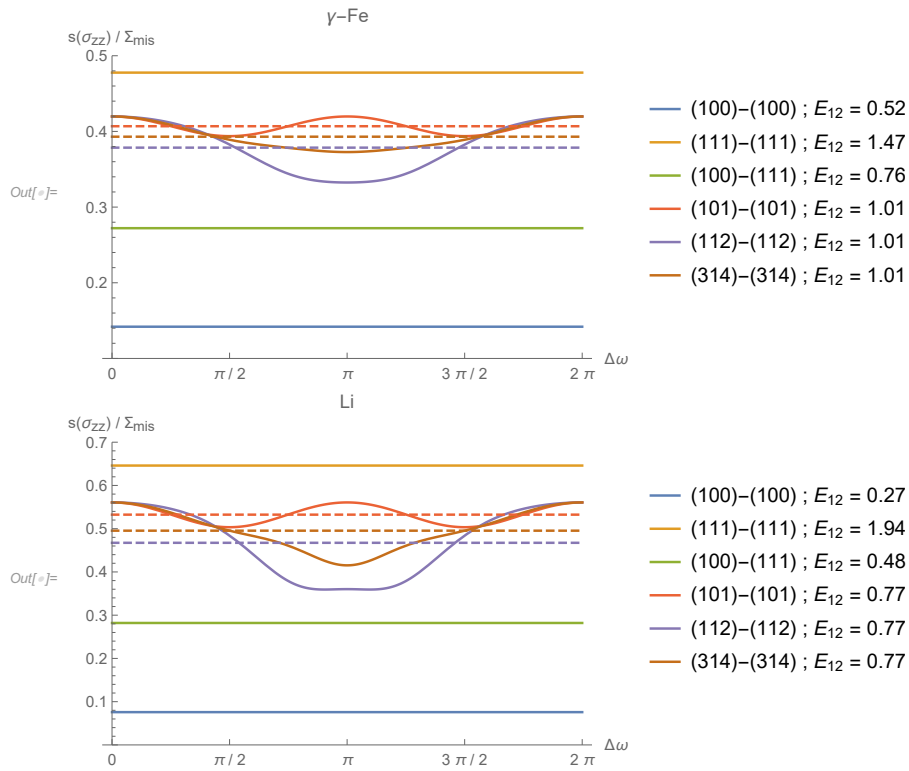


Figure 3: Standard deviation of  $\sigma_{zz}$  distribution as a function of twist-angle difference  $\Delta\omega := \omega_2 - \omega_1$  for two selected cubic materials and six different GB types. Dashed lines represent the twist-angle averaged values.

## ACKNOWLEDGMENTS

The authors gratefully acknowledge financial support by Slovenian Research Agency (grant P2-0026).

## REFERENCES

- [1] S. El Shawish, T. Mede, and J. Hure. A single grain boundary parameter to characterize normal stress fluctuations in materials with elastic cubic grains. *European Journal of Mechanics - A/Solids*, 89:104293, 2021.
- [2] S. El Shawish and T. Mede. Grain boundary stresses in elastic materials. *arXiv preprint arXiv:2207.11060*, 2022.